Nanoscale

Accepted Manuscript

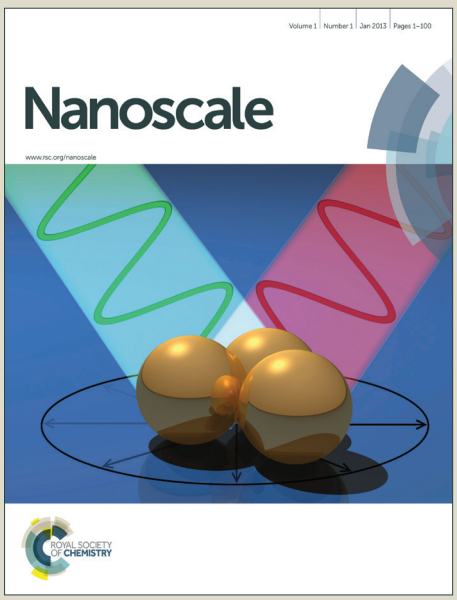

This is an *Accepted Manuscript*, which has been through the Royal Society of Chemistry peer review process and has been accepted for publication.

Accepted Manuscripts are published online shortly after acceptance, before technical editing, formatting and proof reading. Using this free service, authors can make their results available to the community, in citable form, before we publish the edited article. We will replace this *Accepted Manuscript* with the edited and formatted *Advance Article* as soon as it is available.

You can find more information about *Accepted Manuscripts* in the Information for Authors.

Please note that technical editing may introduce minor changes to the text and/or graphics, which may alter content. The journal's standard Terms & Conditions and the Ethical guidelines still apply. In no event shall the Royal Society of Chemistry be held responsible for any errors or omissions in this *Accepted Manuscript* or any consequences arising from the use of any information it contains.

ROYAL SOCIETY OF CHEMISTRY

www.rsc.org/nanoscale

Nanoscale

RSCPublishing

COMMUNICATION

Chemically Exfoliated ReS_2 Nanosheets†

Cite this: DOI: 10.1039/xoxxoooooox

Takeshi Fujita[a], Yoshikazu Ito[a], Yongwen Tan[a], Hisato Yamaguchi[b], Daisuke Hojo[a], Akihiko Hirata[a], Damien Voiry[c], Manish Chhowalla[c], Mingwei Chen[a,d]

Received ooth January 2012,
Accepted ooth January 2012

DOI: 10.1039/xoxxoooooox

www.rsc.org/

The production of two-dimensional rhenium disulfide (ReS_2) nanosheets by exfoliation using lithium intercalation is demonstrated. The vibrational and photoluminescence properties of the exfoliated nanosheets are investigated, and the local atomic structure is studied by scanning and transmission electron microscopy. The catalytic activity of the nanosheets in a hydrogen evolution reaction (HER) is also investigated. The electrochemical properties of the exfoliated ReS_2 nanosheets include low overpotentials of ~100 mV and low Tafel slopes of 75 mV dec^{-1} for HER and are attributed to the atomic structure of the superlattice 1T′ phase. The presence of bandgap photoluminescence demonstrates that the nanosheets retain their semiconducting nature. ReS_2 nanosheets produced by this method provide unique photocatalytic properties that are superior to those of other two-dimensional systems.

The transition-metal dichalcogenide (TMD) family is composed of compounds with the formula MX_2, where "M" is a transition metal from groups 4–10 and "X" is a chalcogen. Thanks to recent developments in graphene technology, layered TMDs have received much attention for their versatile chemistry and applications in a variety of fields, including catalysis, energy storage, sensing, and electronic devices.[1–13] Chemical exfoliation from bulk materials is an effective TMD production method, and liquid exfoliation provides scalable production of thin films and composites.[1,14,15] Lithium intercalation of bulk materials is a well-known and effective exfoliation technique,[16,17] and in group-6 TMDs a transformation from the semiconductor phase (2H: hexagonal structure) to the metallic phase (1T: octahedral structure) is induced during lithium intercalation and exfoliation.[18,19] In addition, the 2H → 1T phase transformation is accompanied by an improvement in catalytic activity. Recent studies showed that metallic exfoliated MoS_2 and WS_2 nanosheets exhibit excellent catalytic performance in hydrogen evolution reactions (HERs).[20-24] However, the practical availability of other systems is very limited, and to the best of our knowledge chemical exfoliation of ReS_2 has not been demonstrated previously.

In this study, we produced chemically exfoliated ReS_2 nanosheets from bulk powders using a solvent-free method involving Li. The local atomic structure of the nanosheets was investigated using transmission electron microscopy (TEM), atomic force microscopy (AFM), and X-ray photoelectron spectroscopy (XPS); in addition, we studied their vibrational properties, photoluminescence (PL), and catalytic activity in HERs. The production of ReS_2 nanosheets by liquid or chemical exfoliation has not been reported previously in literature,[1,14,15] and the ability of Li intercalation to produce ReS_2 nanosheets is largely unknown. We found that a solvent-free method[25] involving the reaction of ReS_2 powder with lithium borohydride ($LiBH_4$) is effective for intercalating Li, and this method could replace the conventional protocol involving a butyl lithium solution.[16] The common butyl lithium reagent did not work well for the exfoliation in this study. The results suggest that the butyl lithium reagent may not be efficient enough to intercalate between the ReS_2 layers to obtain sufficient yield of exfoliation via the chemical route.

The surface morphology of the as-received ReS_2 powders was investigated using scanning electron microscopy (SEM), and the SEM images are shown in Figure 1a. The grain size varied from 100–500 nm, and some grains showed layered filaments. X-ray diffraction data from as-received ReS_2 and Li_xMoS_2 in powder form were collected and are shown in Figure S4 in the Electronic Supporting Information (ESI†). The crystal structure change was confirmed, but no significant change in interlayer spacing was observed. These trends were different from those present in MoS_2 and Li_xMoS_2,[26] therefore the intercalation mechanism of Li in ReS_2 requires further investigation. Figure 1b shows as-exfoliated ReS_2 nanosheets whose size, 50–100 nm, was much smaller than the initial grain size. (Figure S1 in the ESI† shows additional low-magnification scanning TEM (STEM) images indicating their morphology and quality.) Figure 1c is a photograph of a typical dark-brown suspension of chemically exfoliated ReS_2 in water. The AFM results indicated that the average thickness of an exfoliated nanosheet was ≈2.3 nm; this thickness corresponds to that of a bilayer because the expected monolayer thickness is ~1 nm,[26] as shown in Figure S3 in the ESI†. Some of nanosheets were exfoliated down to monolayers, a fact confirmed by high-angle annular dark-field STEM (HAADF STEM). Images from monolayer regions (Figures 1d and e)

Nanoscale Accepted Manuscript

showed the characteristic superlattice of the 1T′ phase, which we previously observed in MoS_2 and WS_2 monolayers produced by lithium intercalation, as well as a maze-like pattern of chained clusters.[20,21] The original crystal structure of ReS_2 is a distorted 1T structure with chains of Re clusters.[27-29] The particularly large gain in the d^3 electron count of Re coincides with the fact that the distortion is energetically favorable.[30] However, a salient difference from the original structure is that the Re_4 clusters[31] tend to be more clearly separated from each other; greater Jahn–Teller distortion is therefore expected in ReS_2 nanosheets. The XPS measurements also confirm the structural changes after the exfoliation (see Figure S5 in the ESI†). Moreover, the zeta potentials of the ReS_2 nanosheets are 10 mV lower than that of their bulk counterpart (see Table S2 in the ESI†). After annealing the exfoliated ReS_2 nanosheets at 500 °C for 1 h, the original crystal structure recovered; the 1T structure with chains of Re clusters was confirmed by HAADF STEM imaging, as shown in Figure S2 in the ESI†.

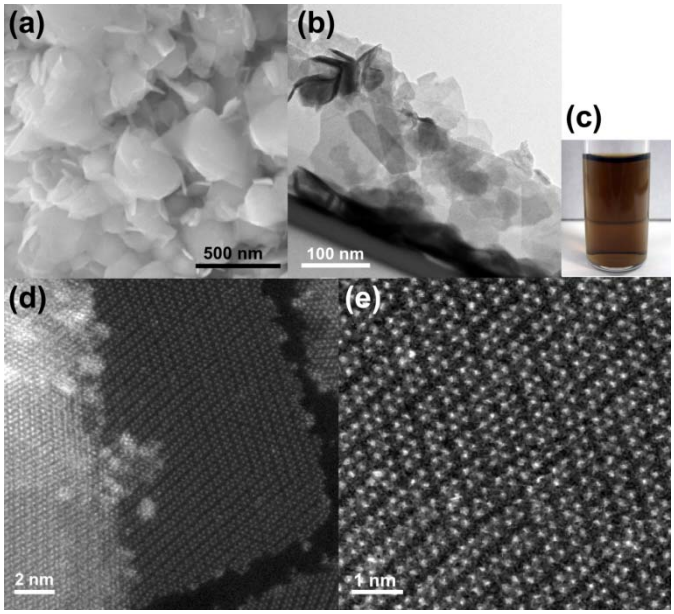

Fig. 1. (a) SEM image of as-received ReS_2 powders, (b) TEM image of as-exfoliated ReS_2 nanosheets, (c) photograph of a typical dark-brown exfoliated ReS_2 suspension in water, (d) high-resolution STEM image of as-exfoliated ReS_2 nanosheets, (e) enlarged STEM image from (d), showing the 1T′ superlattice phase of Re_4 clusters.

We measured the Raman spectra of the as-exfoliated ReS_2 nanosheets and as-received powders, and the results are shown in Figure 2. Because of the small size of the nanosheets, a comprehensive study on the dependence of the optical properties on the stack thickness could not be pursued. Raman spectra were acquired from the restacked nanosheets because the individual nanosheets are small and invisible under an optical microscope. The spectra were acquired several times from thick and thin re-aggregated areas, and there was no significant peak shift in the spectra between the ReS_2 nanosheets and the bulk material. The phonon dispersion of the nanosheets was nearly identical to that of the bulk. A recent theoretical study showed that bulk ReS_2 behaves as electronically and vibrationally decoupled monolayers stacked together; Jahn–Teller distortion of the 1T structure prevents ordered stacking and minimizes the interlayer overlap of wavefunctions.[28] This vibrational decoupling seems to be present not only in mechanically exfoliated nanosheets but also in chemically exfoliated ones. The peak near 150 cm^{-1} assigned to the E_g mode was different from that found in ref. 28. The difference may come from the differences of excitation laser wavelengths of 488 nm in ref. 28 and 512 nm in this study. Also, the in-plane motion in ReS_2 may be sensitive to the crystallinity; the starting powders in this study were commercially supplied and the material in ref. 28 was synthesized by a chemical vapor transport technique, resulting in a large single crystal.

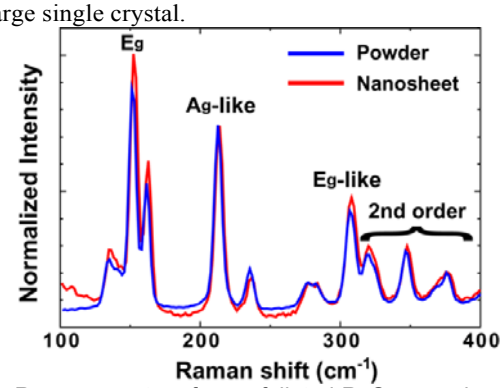

Fig. 2. Raman spectra of as-exfoliated ReS_2 nanosheets and as-received powders. The phonon dispersion of the ReS_2 nanosheets is nearly identical to that of the bulk material.

In order to evaluate whether ReS_2 remains semiconducting or becomes metallic after chemical exfoliation, we investigated the PL properties of as-exfoliated samples. Figure 3 shows PL spectra from the re-stacked nanosheets on a Si substrate. In sharp contrast to the cases of MoS_2 and WS_2,[21,26] as-synthesized ReS_2 nanosheets exhibit significant PL. In the thin and well-dispersed area shown in Figure S6 in the ESI†, a weak PL spectrum was obtained, and the 1T′ phase of ReS_2 retained its semiconducting nature. Distortion of the Re atom arrangement from perfect hexagonal symmetry creates a distortion of the S atom arrangement both perpendicular and parallel to the basal plane. This distortion opens an energy band gap due to mutual repulsion of the orbitals around the Fermi level.[30]

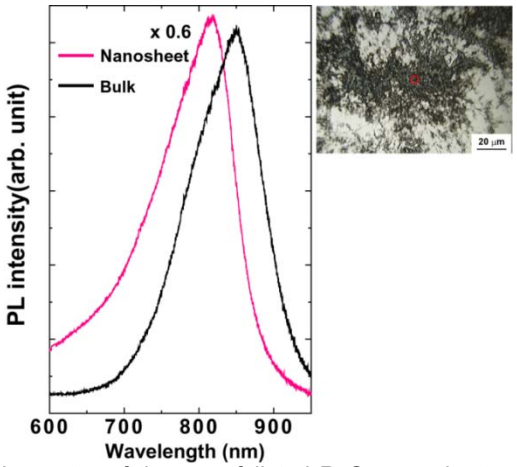

Fig. 3. PL spectra of the as-exfoliated ReS_2 nanosheets on an oxidized Si substrate. The optical microscope images show the analyzed area (red circles). The spectrum from the bulk (as-received powders) is shown for comparison.

Moreover, we could not find any intense PL signals, unlike the case with MoS_2.[32-34] The ReS_2 nanosheets did not show hot

Nanoscale Accepted Manuscript

This journal is © The Royal Society of Chemistry 2012

luminescence from indirect-to-direct bandgap transitions or any dependence of PL on the number of layers. Although it was difficult to control the thickness of the ReS_2 nanosheets on the substrate in order to investigate the influence of layer thicknesses on PL, intense peaks were obtained only from the aggregated areas in Figures 3 and S6 in the ESI†, both of which were at 810 nm (1.53 eV). The stronger peaks are closely related to the increased volume/area of the probed regions. A blue shift is observed after exfoliation in comparison with the peak from bulk ReS_2 (as-received powders) at 850 nm (1.45 eV). The physical origin of this shift is unclear, but these trends in PL are in good agreement with previous results with mechanically exfoliated samples[28] and other TMDs.[35] Quantum size effects may also contribute to the blue shift.

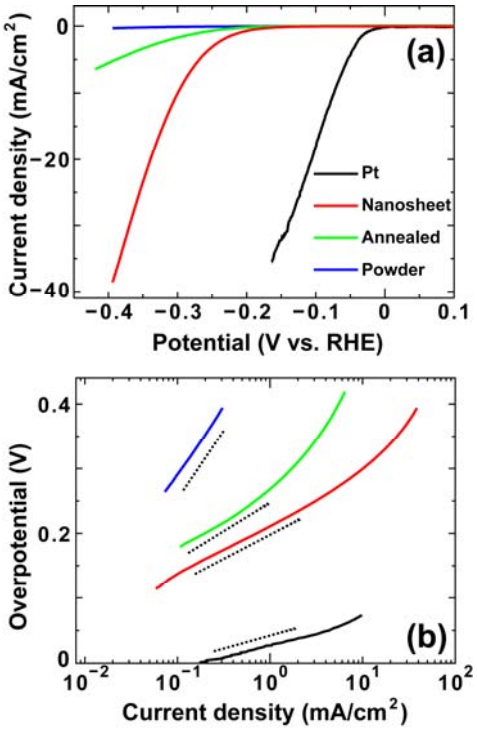

Fig. 4. HER electrocatalytic properties of exfoliated ReS_2 nanosheets: (a) polarization curves of ReS_2 nanosheets—as-exfoliated and after annealing at 500 °C—and Pt nanoparticles and as-received ReS_2 powders for comparison, (b) corresponding Tafel plots obtained from the polarization curves, showing slopes of 75 and 88 mV dec^{-1} for the as-exfoliated and annealed ReS_2 nanosheets, respectively. There is significant reduction in the Tafel slope for exfoliated samples as compared to as-received powder samples. The dashed lines represent the slope for each sample.

We also investigated the HER catalyst performance of the chemically exfoliated 1T′ phase of ReS_2. Figure 4a compares the HER polarization curves for as-exfoliated and annealed (500 °C) ReS_2 nanosheets, as-received ReS_2 powders, and conventional Pt nanoparticles as a reference (all data not *iR* corrected). HER activity was dramatically enhanced in the as-exfoliated 1T′ nanosheets as compared to their annealed 1T counterpart and the bulk material. Tafel plots derived from these data are shown in Figure 4b; the linear portions of the data in Figure 4b were fitted to the Tafel equation to determine the slopes (dashed lines), and these were used to determine the overpotential of the electrochemical reaction. The Tafel plots reveal slopes of 75 mV dec^{-1} for the as-exfoliated ReS_2 nanosheets, 88 mV dec^{-1} for the annealed ReS_2 nanosheets, 211 mV dec^{-1} for the as-received powders, and 37 mV dec^{-1} for the Pt nanoparticles, indicating reduced overpotential in the nanosheets. The Tafel plot of the as-exfoliated ReS_2 nanosheets is comparable with the results of our previous study on as-exfoliated WS_2 nanosheets,[20] and it exhibits slightly higher values than other nanostructured MoS_2 materials such as MoS_2 nanoparticles on highly conductive reduced graphene oxide[36] and exfoliated 1T MoS_2 nanosheets.[21,22]

In our previous study of chemically exfoliated WS_2 and MoS_2,[20,21] we found that regions of the metallic phase induced by local strains acts as active sites for enhanced HER. Experimental results suggest that a similar scenario can be applied to the as-exfoliated ReS_2 nanosheets as the 1T′ superlattice phase, shown in Figures 1d and e, can be considered as a "strained" 1T phase. This explanation for enhanced HER in as-exfoliated ReS_2, resulting from improved electrical conductivity from local strains, is consistent with it possessing the lowest overpotential of ~100 mV (Figure 4b) and the lowest Tafel slope among the ReS_2 materials investigated in this study. After annealing at 500 °C, the metastable 1T′ phase relaxes to the ground-state 1T phase (Figure S2, ESI†), losing its improved electrical conductivity; it has fewer active sites, a higher overpotential of ~200 mV, and a higher Tafel slope. These results suggest the origin of the high catalytic activity of metastable-phase TMDs such as the 1T phase of WS_2 and MoS_2. The high catalytic performance of as-exfoliated ReS_2 combined with the unique intrinsic band gap that is evident in the PL data (chemically exfoliated MoS_2 and WS_2 are metallic thus do not exhibit PL) indicate materials properties that are promising for realizing highly active TMD photocatalysts without the need for photocatalytic materials such as TiO_2, which are currently essential.[37]

Electrochemical stability is important to the viability of a HER catalyst. In order to investigate the stability of these materials under electrocatalytic operation, we have measured the HER characteristics of the metastable 1T′ electrodes by subjecting them to over 1,100 cycles and monitoring the current density at –0.3 V, as shown in Figure 5. The current density shows slight degradation to 70% of its original value after 1,000 cycles, which might be caused by the consumption of H^+ or strain relaxation in the 1T′ phase. The cycling stability of the metastable 1T′ electrodes is expected to be further improved by modifying the electrode with an effective current collector.[21]

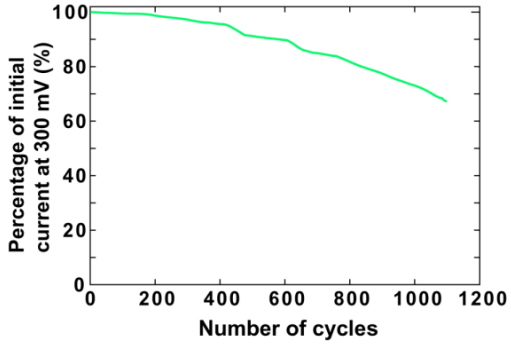

Fig. 5. Cycling stability of the metastable 1T′ electrodes at a constant overpotential of 300 mV.

Conclusions

In summary, we have established a synthesis route for chemically exfoliated ReS_2 nanosheets starting from powders. These nanosheets show high HER activity originating from the

Nanoscale Accepted Manuscript

1T′ superlattice phase, and they also maintain their semiconducting properties, as demonstrated by PL results. ReS_2 nanosheets may therefore fulfill roles in photocatalysis that other 2D systems cannot play. The ReS_2 nanosheets may also be useful for other catalysis applications, such as sulfur-tolerant hydrogenation and hydrodesulfurization.[38,39]

Acknowledgements

This work was supported by JSPS, Grant-in-Aid for Challenging Exploratory Research (24656028), Scientific Research on Innovative Areas "Science of Atomic Layers" (90363382).

Notes and references

[a] *WPI Advanced Institute for Materials Research, Tohoku University, Sendai 980-8577, Japan.*
E-mail tfujita@wpi-aimr.tohoku.ac.jp or mwchen@wpi-aimr.tohoku.ac.jp.
[b] *MPA11 Materials Synthesis and Integrated Devices (MSID), Materials Physics and Applications (MPA) Division, Mail Stop: K763, Los Alamos National Laboratory (LANL), P.O. Box 1663, Los Alamos, NM 87545, U.S.A.*
[c] *Materials Science and Engineering, Rutgers University, 607 Taylor Road, Piscataway, NJ 08854, U.S.A.*
[d] *State Key Laboratory of Metal Matrix Composites, School of Materials Science and Engineering, Shanghai Jiao Tong University, Shanghai 200030, PR China.*
† Electronic Supplementary Information (ESI) available: [Experimental procedures for sample synthesis and characterization]. See DOI: 10.1039/c000000x/

1 V. Nicolosi, M. Chhowalla, M. G. Kanatzidis, M. S. Strano and J. N. Coleman, *Science*, 2013, **340**, 1226419.
2 M. Chhowalla, H. S. Shin, G. Eda, L. J. Li, K. P. Loh and H. Zhang, *Nat. Chem.*, 2013, **5**, 263.
3 G. Eda and S. A. Maier, *ACS Nano*, 2013, **7**, 5660.
4 C. N. R. Rao, H. S. S. R. Matte and U. Maitra, *Angew. Chem. Int. Ed.*, 2013, **52**, 13162.
5 H. Li, J. M. T. Wu, Z. Y. Yin and H. Zhang, *Acc. Chem. Res.*, 2014, **47**, 1067.
6 X. Huang, C. L. Tan, Z. Y. Yin and H. Zhang, *Adv. Mater.*, 2014, **26**, 2185
7 X. Huang, Z. Y. Zeng and H. Zhang, *Chem. Soc. Rev.*, 2013, **42**, 1934.
8 Z. Y. Zeng, C. L. Tan, X. Huang, S. Y. Bao and H. Zhang, *Energy Environ.Sci.*, 2014, **7**, 797.
9 Z. Y. Yin, H. Li, H. Li, L. Jiang, Y. M. Shi, Y. H. Sun, G. Lu, Q. Zhang, X. D. Chen and H. Zhang, *ACS Nano*, 2012, **6**, 74.
10 X. H. Cao, Y. M. Shi, W. H. Shi, X. H. Rui, Q. Y. Yan, J. Kong and H. Zhang, *Small*, 2013, **9**, 3433.
11 C. F. Zhu, Z. Y. Zeng, H. Li, F. Li, C. H. Fan and H. Zhang, *J. Am. Chem. Soc.*, 2013, **135**, 5998.
12 H. Li, Z. Y. Yin, Q. Y. He, H. Li, X. Huang, G. Lu, D. W. H. Fam, A. I. Y. Tok, Q. Zhang and H. Zhang, *Small*, 2012, **8**, 63.
13 X. Huang, Z. Y. Zeng, S. Y. Bao, M. F. Wang, X. Y. Qi, Z. X. Fan and H. Zhang, *Nat. Commun.*, 2013, **4**, 1444.
14 J. N. Coleman, M. Lotya, A. O'Neill, S. D. Bergin, P. J. King, U. Khan, K. Young, A. Gaucher, S. De, R. J. Smith, I. V. Shvets, S. K. Arora, G. Stanton, H. Y. Kim, K. Lee, G. T. Kim, G. S. Duesberg, T. Hallam, J. J. Boland, J. J. Wang, J. F. Donegan, J. C. Grunlan, G. Moriarty, A. Shmeliov, R. J. Nicholls, J. M. Perkins, E. M. Grieveson, K. Theuwissen, D. W. McComb, P. D. Nellist and V. Nicolosi, *Science*, 2011, **331**, 568.
15 J. Zheng, H. Zhang, S. H. Dong, Y. P. Liu, C. T. Nai, H. S. Shin, H. Y. Jeong, B. Liu and K. P. Loh, *Nat. Commun.*, 2014, **5**. 2995.
16 P. Joensen, R. F. Frindt and S. R. Morrison, *Mater. Res. Bull.*, 1986, **21**, 457.
17 Z. Y. Zeng, Z. Y. Yin, X. Huang, H. Li, Q. Y. He, G. Lu, F. Boey and H. Zhang, *Angew. Chem. Int. Ed.*, 2011, **50**, 11093.
18 M. A. Py and R. R. Haering, *Can. J. Phys.*, 1983, **61**, 76.
19 L. F. Mattheis, *Phys. Rev. B*, 1973, **8**, 3719.
20 D. Voiry, H. Yamaguchi, J. W. Li, R. Silva, D. C. B. Alves, T. Fujita, M. W. Chen, T. Asefa, V. B. Shenoy, G. Eda and M. Chhowalla, *Nat. Mater.*, 2013, **12**, 850.
21 D. Voiry, M. Salehi, R. Silva, T. Fujita, M. W. Chen, T. Asefa, V. B. Shenoy, G. Eda and M. Chhowalla, *Nano Lett.*, 2013, **13**, 6222.
22 M. A. Lukowski, A. S. Daniel, F. Meng, A. Forticaux, L. S. Li and S. Jin, *J. Am. Chem. Soc.*, 2013, **135**, 10274.
23 M. A. Lukowski, A. S. Daniel, C. R. English, F. Meng, A. Forticaux, R. J. Hamers and S. Jin, *Energy Environ. Sci.*, 2014, **7**, 2608.
24 Q. Ding, F. Meng, C. R. English, M. Cabán-Acevedo, M. J. Shearer, D. Liang, A. S. Daniel, R. J. Hamers and S. Jin, *J. Am. Chem. Soc.*, 2014, **136**, 8504.
25 H. L. Tsai, J. Heising, J. L. Schindler, C. R. Kannewurf and M. G. Kanatzidis, *Chem. Mater.*, 1997, **9**, 879.
26 G. Eda, H. Yamaguchi, D. Voiry, T. Fujita, M. W. Chen and M. Chhowalla, *Nano Lett.*, 2011, **11**, 5111.
27 H. J. Lamfers, A. Meetsma, G. A. Wiegers and J. L. deBoer, *J. Alloys Comp.*, 1996, **241**, 34.
28 S. Tongay, H. Sahin, C. Ko, A. Luce, W. Fan, K. Liu, J. Zhou, Y. S. Huang, C. H. Ho, J. Y. Yan, D. F. Ogletree, S. Aloni, J. Ji, S. S. Li, J. B. Li, F. M. Peeters and J. Q. Wu, *Nat. Commun.*, 2014, **5**, 3252.
29 H. H. Murray, S. P. Kelty, R. R. Chianelli and C. S. Day, *Inorg. Chem.*, 1994, **33**, 4418.
30 M. Kertesz and R. Hoffmann, *J. Am. Chem. Soc.*, 1984, **106**, 3453.
31 J. V. Marzik, R. Kershaw, K. Dwight and A. Wold, *J. Solid State Chem.*, 1984, **51**, 170.
32 A. Splendiani, L. Sun, Y. B. Zhang, T. S. Li, J. Kim, C. Y. Chim, G. Galli and F. Wang, *Nano Lett.*, 2010, **10**, 1271.
33 K. F. Mak, C. Lee, J. Hone, J. Shan and T. F. Heinz, *Phys. Rev. Lett.*, 2010, **105**, 136805.
34 T. Korn, S. Heydrich, M. Hirmer, J. Schmutzler and C. Schüller, *Appl. Phys. Lett.*, 2011, **99**, 102109.
35 H. R. Gutiérrez, N. Perea-López, A. L. Elías, A. Berkdemir, B. Wang, R. Lv, F. López-Urías, V. H. Crespi, H. Terrones and M. Terrones, *Nano Lett.*, 2013, **13**, 3447.
36 Y. G. Li, H. L. Wang, L. M. Xie, Y. Y. Liang, G. S. Hong and H. J. Dai, *J. Am. Chem. Soc.*, 2011, **133**, 7296.
37 L. A. King, W. J. Zhao, M. Chhowalla, D. J. Riley and G. Eda, *J. Mater. Chem. A*, 2013, **1**, 8935.
38 H. S. Broadbent, L. H. Slaugh and N. L. Jarvis, *J. Am. Chem. Soc.*, 1954, **76**, 1519.
39 T. A. Pecoraro and R. R. Chianelli, *J. Catal.*, 1981, **67**, 430.

Nanoscale Accepted Manuscript

 This journal is © The Royal Society of Chemistry 2012